Journal of Biomaterials and Nanobiotechnology, **2010, 1, 7-16**
doi:10.4236/jbnb.2010.11002 Published Online October 2010 (http://www.SciRP.org/journal/jbnb)

Changes of Surface Composition and Morphology after Incorporation of Ions into Biomimetic Apatite Coatings

Wei Xia[1,2*], Carl Lindahl[1,2], Cecilia Persson[1], Peter Thomsen[2,3], Jukka Lausmaa[2,4], Håkan Engqvist[1,2*]

[1]Materials in Medicine, Applied Materials Science, the Ångstrom Laboratory, Uppsala University, Uppsala, Sweden; [2]Biomatcell, VINN Excellence Center of Biomaterials and Cell Therapy, Gothenburg, Sweden; [3]Institute for Clinical Sciences, Sahlgrenska Academy at University of Gothenburg, Gothenburg, Sweden; [4]Department of Chemistry and Materials Technology, SP Technical Research Institute of Sweden, Borås, Sweden.
Email: {wei.xia@, hakan.engqvist}@angstrom.uu.se

Received July 28th, 2010; revised August 19th, 2010; accepted September 20th, 2010.

ABSTRACT

Incorporating trace elements into apatite coatings may permit the combination of several pharmaceutical effects due to the different ions. In this study, strontium, silicon, and fluoride ions have been incorporated into apatite coatings through a biomineralization method, which mimics an in vitro mineralization process. The surface composition was tested with X-ray diffraction and X-ray photoelectron spectroscopy, and the surface morphology was characterized with scanning electron microscopy. Compared with pure hydroxyapatite coating, the strontium, silicon, and fluoride substituted apatite coatings showed different morphologies, such as spherical, needle-like, and nano-flake-like, respectively. The crystal size of these biomimetic hydroxyapatite coatings decreased after ion substitution. The results of the analysis of surface composition showed an increased amount of the ion substitutions with an increase of ion concentrations in the soaking solution. That means the ion incorporation into the apatite structure based on the biomineralization method could not only vary the ion content but also change the morphology of the apatite coatings. Herein, the role of ion substitution is considered from the point of view of materials science at the micro structural and surface chemistry levels.

Keywords*: *Biomineralization, Hydroxyapatite, Coating, Substitution, Biomimetic

1. Introduction

Surface composition and morphology are two key factors in implant coatings. The outermost layer of a biomaterial's surface possesses different properties depending on its elemental compositions and functionalities (such as -PO_4, -SiOH, -TiOH, -OH, -COOH, and -NH_2 groups). Bioactive silicate glasses can chemically bond with the bone tissue because they can form a SiOH layer on the surface in water solution and induce, further, the formation of hydroxyapatite [1]. Kokubo *et al*. reported that the bioactivity and bone-bonding ability of titanium implants treated with an alkali hydroxide solution have been improved because of the existence of TiOH groups on the surface [2]. Surface topography also affects the bioactivity, biocompatibility, and tissue in-growth [3]. Osteoblast-like cells adhere more readily to and appear more differentiated on rough surfaces [3-5]. Recent studies report that surfaces with specific nano- and micro-topographies can improve the cell adhesion, change the cell spreading, and enhance the gene expression [6-8]. Therefore, the fabrication of bioactive materials presenting surfaces with these types of topographies is of great interest.

Hydroxyapatite (HA), $Ca_{10}(PO_4)_6(OH)_2$, a calcium phosphate found in bone and teeth, presents good osteoconductivity and osteoinductivity and is commonly used in dental and orthopedic surgery [9]. The high biocompatibility of HA has also led to its use as a coating material on metallic implants such as titanium, stainless steel and Co-Cr alloys [10-12]. However, the synthetic HA is still needs to be improved. For example, it has been shown to induce apatite formation at a slower rate than other materials, such as silicate based bioactive glasses [13]. Furthermore, the low resorbability rate of synthetic, stoichiometric hydroxyapatite limits the rate of in-growth for new bone formation [14,15]. These factors may result in an increased risk of implant failure due to the

deficient fixation.

A previous study has shown that the bioactivity and resorbability of hydroxyapatite can be improved by decreasing the crystallinity and introducing ion substitutions in its structure [16]. In fact, it is well known that natural bone mineral is a calcium deficient hydroxyapatite with low crystallinity. Various ionic substitutions, cationic as well as anionic, exist in bone mineral, such as Sr, Si, Mg, CO_3^{2-} and F. Anions can be incorporated into the sites of OH^- (type A) and PO_4^{3-} (type B) [17], and cations can be incorporated into the sites Ca^{2+} I and Ca^{2+} II [18]. These ions also have important functions in the bone. For instance, a reduction in bone resorption and an increase in the mechanical strength may be obtained through Sr substitutions [19,20]. Silicon can increase the bone mineralization rate and enhance the osteopath proliferation, differentiation and collagen production [21]. Fluoride, which is good for teeth, can stabilize apatite and also stimulate the osteoblast activity [22,23]. Finally, previous research has shown that ion substituted apatite materials may improve the interaction between bone and synthetic apatite materials [24].

Methods to fabricate HA and ion substituted coatings include plasma spraying [25], sol-gel [26], magnetron co-sputtering [27], pulsed-laser deposition [28] and micro-arc oxidation techniques [29]. Although these techniques allow the preparation of HA coatings combined with a tailoring of the chemical composition, the draw- backs of synthetic HA have not been resolved. Recently, a solution method termed the biomineralization method has been used to fabricate biomimetic HA coatings on implants [3, 30-32]. This biomimetic method maintains low deposition temperatures and also provides a good surface coverage of complex geometrical shapes. The obtained coating is calcium deficient, not completely crystallized and the chemical composition can be tailored using different ions. *In vivo* studies show that this apatite coating provides faster new bone in-growth and coating resorbability in early bone formation [33]. However, a histological study found that rough titanium implants had a more positive effect on new bone formation than the biomimetic apatite coating [34].

In brief, there is room for improvement of this biomimetic coating in order to strengthen the implant and bone bonding and to have a stronger positive effect on new bone formation. Previous work suggests that the surface composition and the topography of the coatings are key parameters affecting the bioactivity, biocompatibility, and further material/tissue interactions such as tissue ingrowth. In this work, we prepared ion substituted (Sr, Si, F) apatite (*i*HA) coatings with varied compositions and surface morphology on pre-treated titanium substrates through a biomineralization method.

2. Materials and Methods

2.1. Materials

Pure titanium (Grade 2, 99.4% pure, Edstraco AB, Sweden) cut as squares (10x10mm, with a 1mm thickness) was used as a substrate for the biomimetic coatings. The base soaking medium was phosphate buffer solution (Dulbecco's PBS, Aldrich, USA). The ion composition of this PBS is: Na^+ (145mM), K^+ (4.3mM), Mg^{2+} (0.49mM), Ca^{2+} (0.91mM), Cl^- (143mM), and HPO_4^{2-} (9.6mM).

2.2. Surface Treatment

Crystalline titanium dioxides have been proven to strengthen the physical–chemical bonding between the implants and living bones because of their ability to induce a bone-like apatite in the body's environment [35]. Therefore, such oxidized Ti surface could be considered as a good transition layer on the Ti-based implant's surface. In this study, a titanium oxide layer was created on the titanium plates in the form of a rutile film via a thermal oxidation process. Ti plates were treated at 800℃ for 1 hour with a ramping rate of 5℃/min. Thereafter the plates were treated with an alkaline solution (1M NaOH) and ethanol in an ultrasonic bath before use.

2.3. Biomimetic Ion Substituted Apatite Coating Deposition

The preparation of the biomimetic ion substituted apatite coating was performed in an ion modified PBS solution. The initial pH value is 7.4, adjusted by NaOH and HCl solutions. In order to investigate which factors that influence the biomimetic coating deposition, a series of ion concentrations and soaking times were studied. Sr, Si and F ion concentrations were varied between 0.06mM and 0.6 mM, 0.075 mM and 0.15 mM, 0.04 mM and 0.2 mM, respectively, and soaking time from 12 hours to 2 weeks. The maximum concentrations used for the different ions were limited by the precipitation of the same at higher concentrations. All specimens were soaked in 40 ml preheated solution in sealed plastic bottles, which were then stored in an oven at 37℃. The solution was exchanged every 3 days to avoid depletion of calcium and phosphate ions. All samples were rinsed with de-ionized water and dried at 37℃ prior to characterization.

2.4. Morphological and Chemical Characterization

The morphology of the specimens before and after coating was evaluated using field emission scanning electron microscopy (FE-SEM, LEO 1550). An SE2 detector was used with an accelerating voltage of 10 kV. The crystallinity of the specimens was analyzed using X-ray

diffractometry (TF-XRD, Siemens Diffractometer 5000) using Cu Ka radiation (k = 1.5418 Å). The diffractometer was operated at 45 kV and 40 mA at a 2 h range of 10–80°, with a fixed incidence angle of 1°. The chemical composition was analyzed by X-ray photoelectron spectroscopy (XPS, Physical Electronics Quantum 2000, Al Kα X-ray source).

2.5. Estimation of Crystal size and Crystallinity

This estimation method was referred from Li *et al* [18]. The size of HA and Sr, Si and F-HA crystals were calculated from XRD data using the Scherrer equation. The peak of (002) was fit to define the full width at half maximum intensity (FWHM):

$$d = \frac{k\lambda}{FWHM \bullet \cos\theta} \quad (1)$$

Where d is the crystal size, λ is the wavelength of Cu K_α radiation (λ = 1.5418Å), and k is the broadening constant varying with crystal habit and chosen as 0.9 for the elongated apatite crystallites.

X_c, the crystallinity, corresponds to the fraction of crystalline apatite phase in the investigated volume of powdered samples. An empirical relation between X_c and the FWHM was deduced, according to the equation:

$$X_c = \left(\frac{K_A}{FWHM}\right)^3 \quad (2)$$

where X_c is the crystallinity degree, K_A is a constant set at 0.24.

3. Results

Figure 1 shows the SEM images of hydroxyapatite (HA)

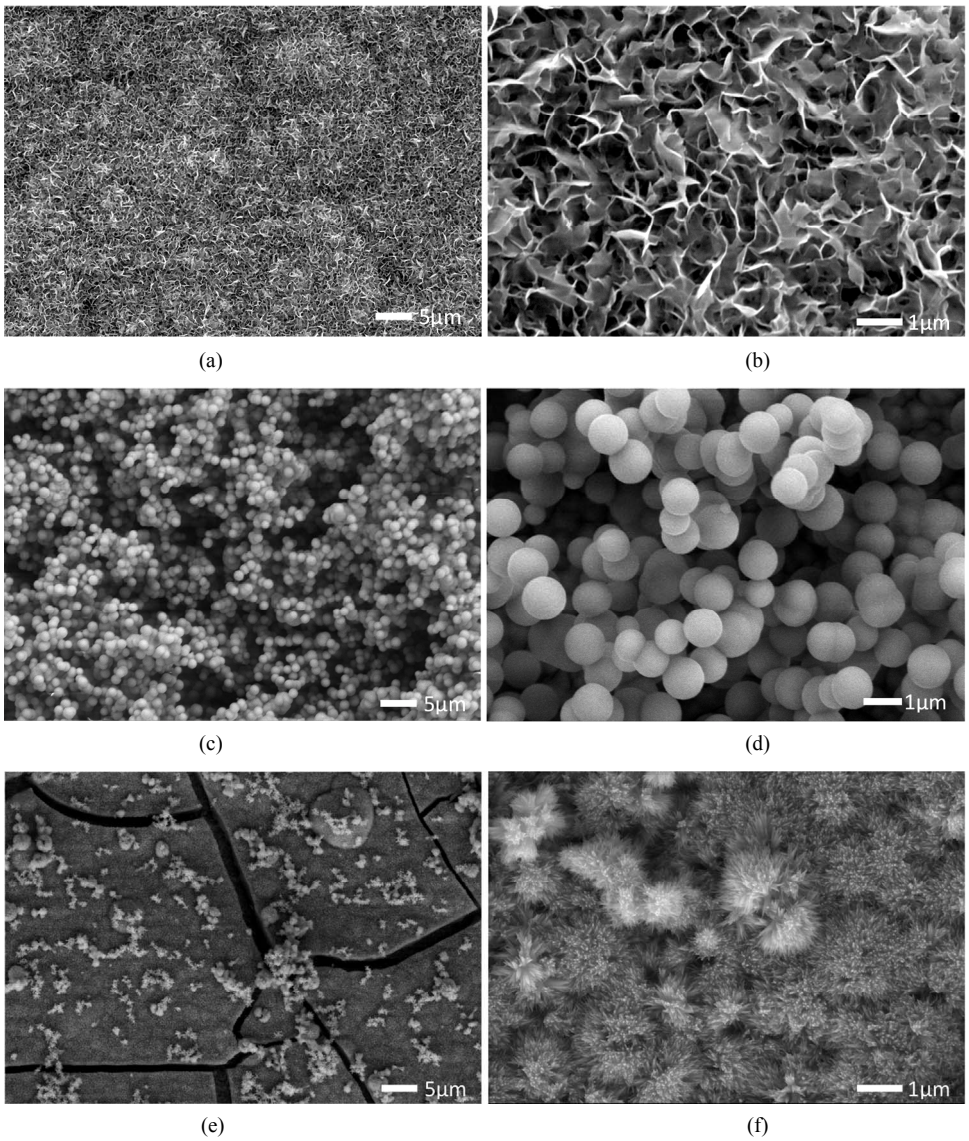

(a) (b)

(c) (d)

(e) (f)

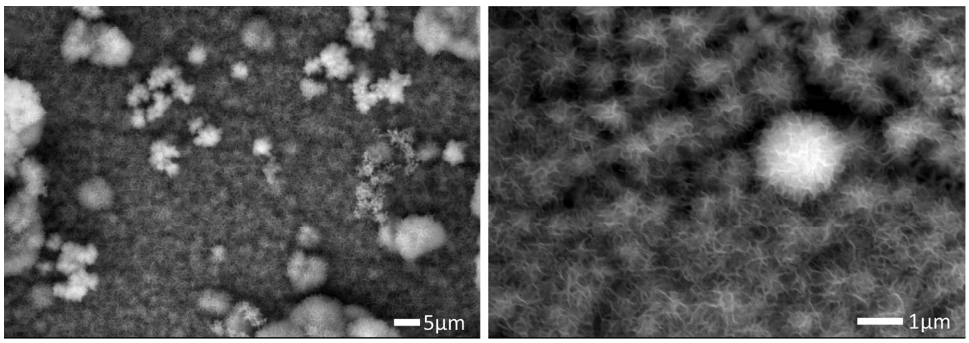

(g) (h)

Figure 1. Surface morphology of the TiO_2/Ti substrates after soaking for 2 weeks in PBS containing different ion concentrations. (a) and (b) no additional ion doped, (c) and (d) 0.6 mM strontium ion doped, (e) and (f) 0.2 mM fluoride ion doped, (g) and (h) 0.15 mM silicate ion doped.

without substituted ions, strontium substituted hydroxylapatite (Sr-HA), fluoride substituted hydroxyapatite (F-HA) and silicon substituted hydroxyapatite (Si-HA) coatings on TiO_2/Ti substrates after soaking in PBS for 2 weeks. It is clear that the morphology strongly depends on the substituted ions. For the pure HA coating (**Figure 1(a)** and **(b)**), it is flake-like, with flakes of approximately 100 nm-1 μm in length and width. The Sr-HA coating (**Figure 1(c)** and **(d)**) has an entirely different morphology with sphere-like particles of approximately 200-800 nm diameter. For the F-HA coating (**Figure 1(e)** and **(f)**), the morphology was again different, presenting a needle-like structure. The morphology of the Si-HA coating (**Figure 1(g)** and **(h)**) was relatively similar to the pure HA coating. It was also flake-like, but the size of the Si-HA particles was much smaller than pure HA; less than 100 nm in length and width. The XRD analysis (**Figure 2**) showed diffraction peaks of apatite in all cases, asdetected around 31º related to the overlapping of planes (211), (112), and (300), and around 26° related to plane (002).

In order to study the influence of the ion concentration on the structure of the HA coating, the results of using lower concentrations of Sr (0.06 mM), Si (0.075 mM) and F (0.02 mM) ions are shown in **Figure 3**. It can be seen that the morphology of the Sr-HA coating still appears sphere-like, although the interface is rougher, porous and with a wider size distribution. However, the decrease in Si and F ion concentration did not greatly affect the morphology of F-HA and Si-HA coatings (**Figure 3(b)** and **(c)**). The F-HA coating was still needle-like, and the Si-HA coating was flake-like with nano-sized particles.

The early formation of the HA coatings, after soaking in PBS for 12 hours, is shown in **Figure 4**. All specimens were soaked in the high concentration ion doped PBS solution. It can be seen that the early Sr-HA coating (**Figure 4(a)**) is a flat layer which is different to the morphology of the coating after soaking for 2 weeks. A few spherical nano-particles have formed on this early layer. These spherical nanoparticles could be considered to be the base of the formation of the second spherical Sr-HA layer. Herein the Sr-HA coating prepared using the biomineralization method is not a simple layer but a hierarchical coating with a gradient structure from a flat and dense early layer to a spherical and porous layer. The early F-HA coating (**Figure 4(b)**) grows from the substrate with needle-like particles. There seems to be no hierarchical structure in the F-HA coating. The early formation of the Si-HA coating (**Figure 4(c)**) shows a nano-sized flake-like layer on the substrate. Again, the structure is similar to the final structure after 2 weeks of soaking.

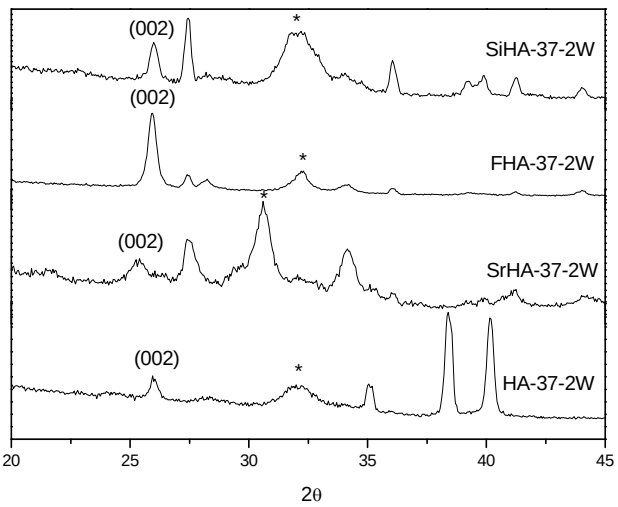

Figure 2. XRD patterns of the HA coatings with and without ion substitution. * and (002): HA. The substrates have been soaked in pure, Sr (0.6 mM), F (0.2 mM) and Si (0.15 mM) PBS for 2 weeks.

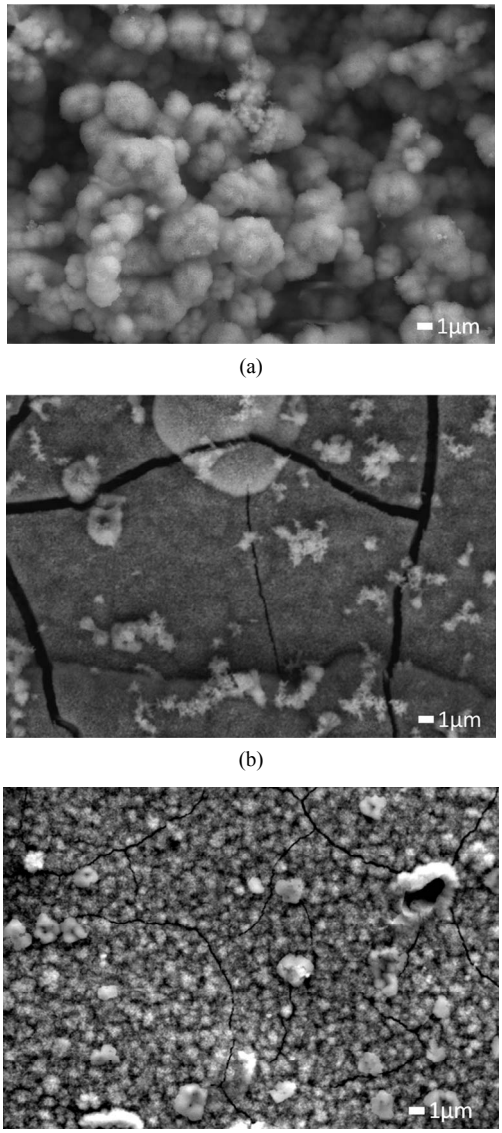

Figure 3. Surface morphology of the TiO2/Ti substrates after soaking for 2 weeks in the lower concentration solutions. (a) 0.06 mM strontium ion doped, (b) 0.04 mM fluoride ion doped, (c) 0.075 mM silicate ion doped.

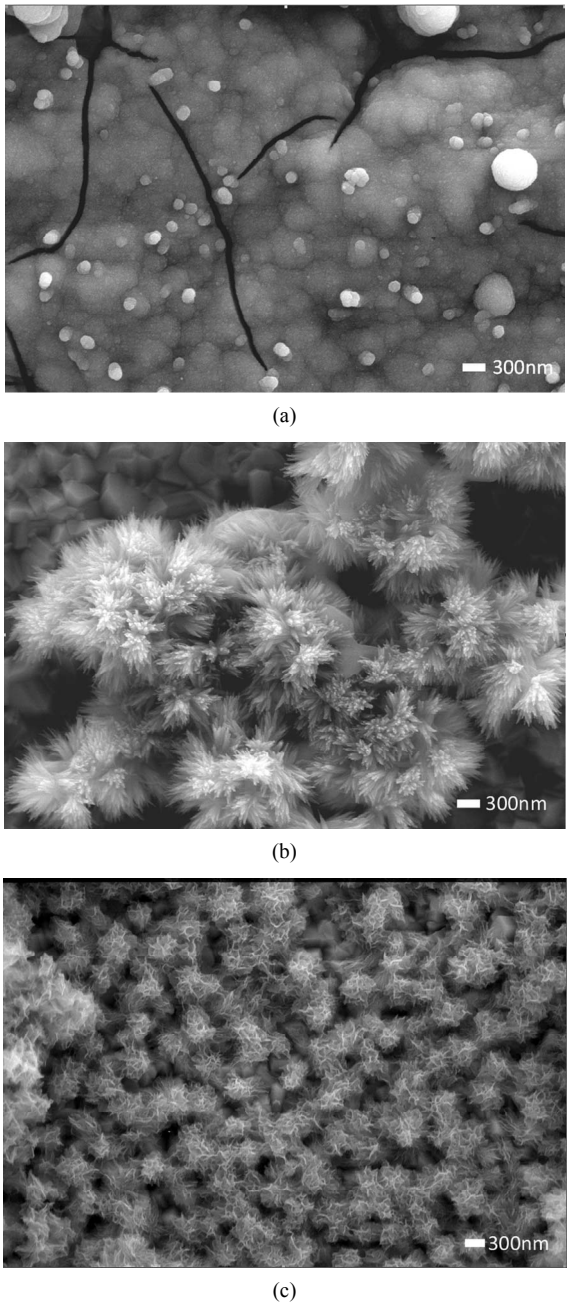

Figure 4. Early growth of ion substituted HA coatings after soaking for 12 hours. (a) strontium (0.6 mM) substituted HA, (b) fluoride (0.2 mM) substituted HA, (c) silicate (0.15 mM) substituted HA.

The changes of crystal size and crystallinity of different apatite coating reflected from the XRD patterns were calculated in order to observe the influence of the Sr, Si and F ions. The (002) reflection was chosen to evaluate the average crystal size because this peak was well resolved and showed no interferences. The d_{002} of HA, SrHA, FHA and SiHA were 35.58, 16.27, 25.10 and 25.45 nm, respectively. The crystal size decreased significantly when hydroxyapatite had been substituted strontium, fluoride and silicon ions. The crystallinity of all HA and Sr, F, and Si substituted HA coatings were very low, just 0.0185, 0.0199, 0.0186 and 0.0185, respectively. That means all of these biomimetic coatings were poorly crysta lliz ed. XPS survey spectra identified calcium, phosphorus, oxygen, strontium, fluoride and silicon as the major constituents of the strontium, fluoride and silicon substituted apatite coating on titanium plates, as expected, see **Figure 5**. All of these spectrums were for the sample prepared at 37℃ for 2 weeks using the higher ion con-

centration. The peak at 134eV (**Figure 5 (a)**) was an overlap of Sr3*d* and P2*p* because Sr3$d_{5/2}$ (133 ± 0.5 eV), Sr3$d_{3/2}$ (135 ± 0.5 eV), P2*p* (132 - 133 eV) lines were closely located. The peak at 684eV (**Figure 5 (b)**) was F1*s*. The weak peak 153eV (**Figure 5 (c)**) was Si2*s*. Si2*p* (~99eV) could not be clearly observed. **Table 1** gives the atomic ratio of the ions in the coatings, obtained from XPS. It can be noted that the composition of the coatings can be varied by changing the ion concentrations in the soaking medium. When the Sr concentration was increased from 0.06 mM to 0.6 mM, the Sr content in the newly formed biomimetic coating increased from 3.56% to 7.74%. The F content in the coating increased from 1.24% to 1.53% after the concentration in PBS was increased from 0.04 mM to 0.2 mM. For the lower Si concentration (0.075 mM), no data was available from the XPS. After the Si concentration was increased to 0.15 mM, 0.56% silicon was found in the coating.

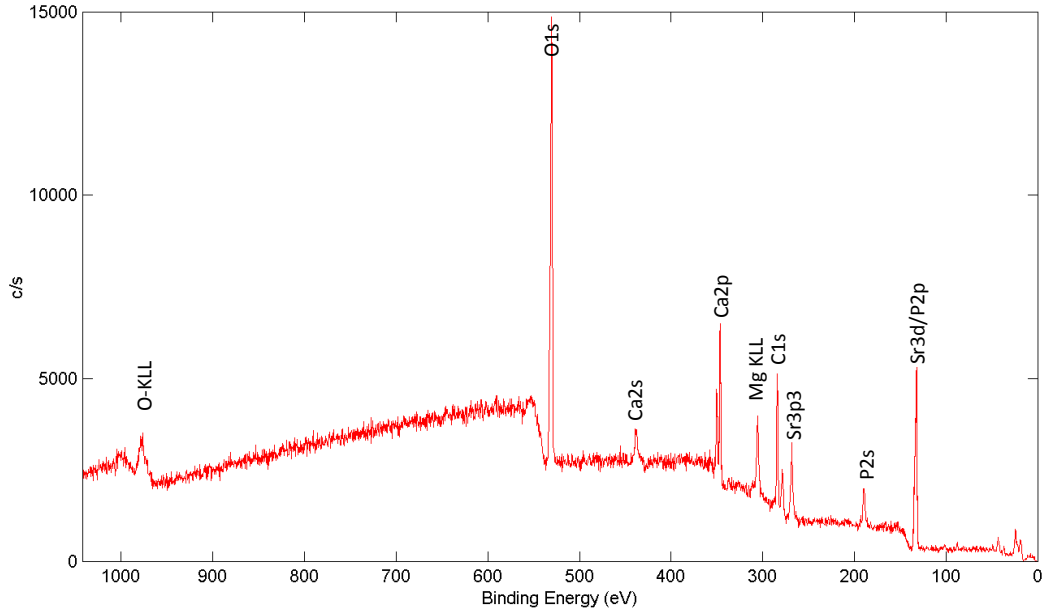

(a)

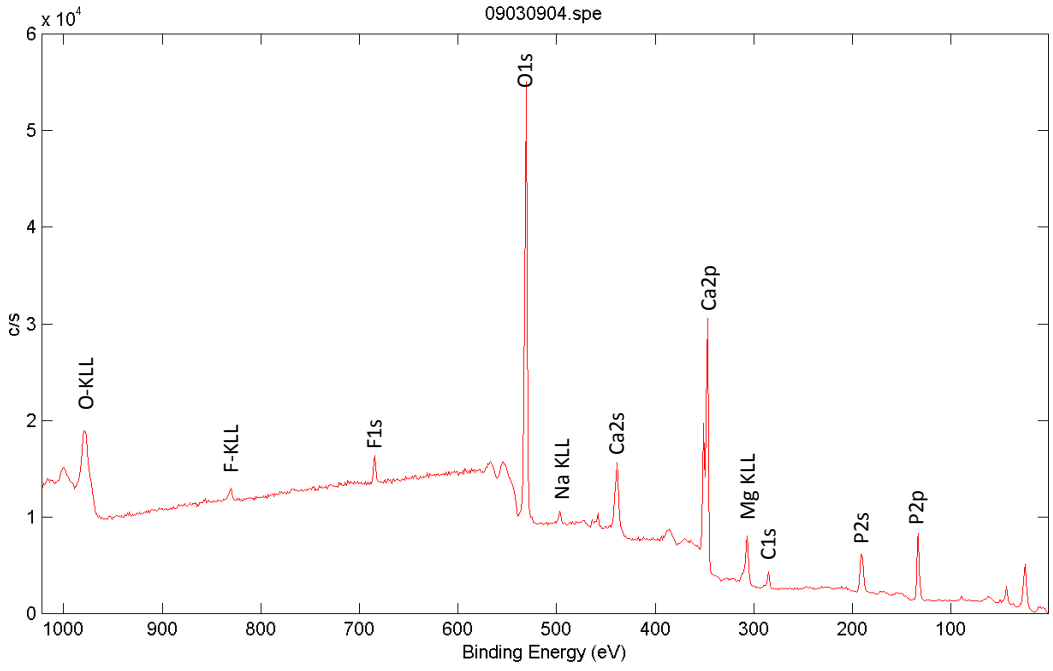

(b)

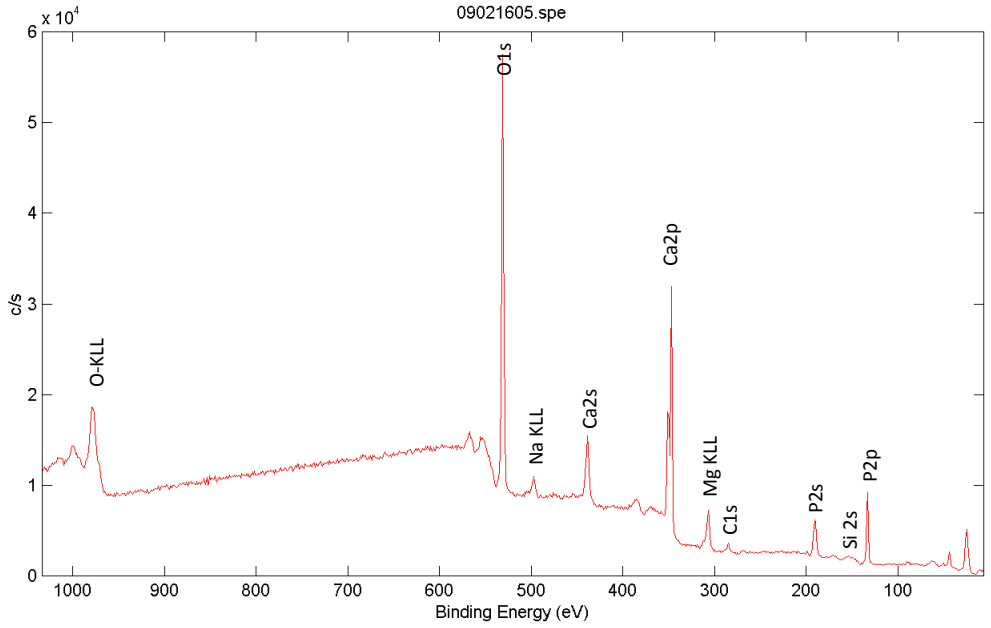

(c)

Figure 5. XPS spectra for strontium (a), fluoride (b), and silicon (c) substituted apatite coating on titanium plates (37℃ for 2 week).

Table 1. Preparation parameters and atomic concentrations of the final coatings. (Error in brackets).

Samples	Ion concentration mM	Temperature ℃	Time week	Substituted ion % of final coating
006SrPBS-37-2W	0.06	37	2	3.56 (1.01)
06SrPBS-37-2W	0.6	37	2	7.74 (1.53)
004FPBS-37-2W	0.04	37	2	1.24 (0.24)
02FPBS-37-2W	0.2	37	2	1.53 (0.11)
0075SiPBS-37-2W	0.075	37	2	-
015SiPBS-37-2W	0.15	37	2	0.56 (0.16)

4. Discussions

In this study it was shown that the topography of hydroxyapatite coatings obtained using a biomineralization method can be varied by adding different ions of varied concentrations to the soaking medium. **Figure 6** gives a schematic illustration of ion substituted hydroxyapatite coatings with different morphologies on the TiO_2/Ti substrates. The non substituted hydroxyapatite coating was composed of flake-like particles in the order of microns. After some of the calcium ions had been replaced by strontium ions, the flake-like coating transformed into a spherical coating with a transitional flat layer. When the OH^- ions were partially replaced by F ions, the new coating had a needle-like morphology. This is very similar to the morphology of tooth enamel [36]. Hydroxyapatite incorporated with fluoride in enamel presents needle-like nanocrystals in highly ordered bundles. Compared with the Sr and F substituted hydroxyapatite coatings, Si substituted hydroxyapatite coating showed a similar morphology to pure hydroxyapatite coating. However, the particle size decreased, from the micrometer to the nanometer scale. These results are different to previously reported HA coatings prepared with solution methods, especially for the Sr-HA and the F-HA coatings [37,38]. Li *et al.* [37] reported on a solution-derived strontium doped apatite coating where the morphology was similar to pure apatite coating even though the strontium concentration reached 1.5 mM. However, in our study the morphology of the Sr-HA coating was completely different to the pure HA coating, even at concentrations as low as 0,06mM Sr. Also, a higher concentration of strontium ions seemed to facilitate the formation of more

spherical particles. Wang *et al*. [38] prepared a F-HA coating using an electrochemical deposition method. They reported that the obtained F-HA particles became sharper and smaller when the F concentration increased in the solution. At certain F concentrations, they could get spindle-like F-HA. Needle-like F-HA exists naturally in tooth enamel [36]. In this study, a well organized needle-like FHA coating was obtained via a mineralization method without an inductor. **Table 2** shows a decrease of the crystal size after hydroxyapatite had been substituted. This reduction in the crystal size of synthetic ion substituted hydroxyapatite was also reported by Li *et al* [18]. The poor crystallinity of the biomimetic coatings has been also reported Bracci and Bigi *et al* [39].

XPS analysis showed that the ion concentration in the soaking solution also influenced the amount of ions substituted into the HA. A higher ion concentration tended to give a higher amount of substituted ions. However, the substitutions we obtained may not be the highest possible substitutions of these ions in hydroxyapatite since, in order to avoid an initial precipitation in PBS solution, higher concentrations of Sr, F and Si ions could not be used. Furthermore, from **Table 1** it can be noted that the amount of substituted ions was highest using strontium, followed by fluoride and finally silicon. This could be due to the differences in initial concentrations of the ions. However, because of the similarity in radius between Sr^{2+} and Ca^{2+} and F^- and OH^-, respectively, the replacement of calcium and hydroxide ions by strontium and fluoride ions is also easier than substituting phosphate by silicate. Since the latter molecules are not single ions they are more difficult to incorporate into hydroxyapatite. Finally, one hydroxyapatite molecule has 10 calcium ions and 2 hydroxide ions. This could allow for more Sr than F substitutions. The resorption rate and the cell response of these ion substituted hydroxyapatite coatings remain to be evaluated and may be of interest for future studies.

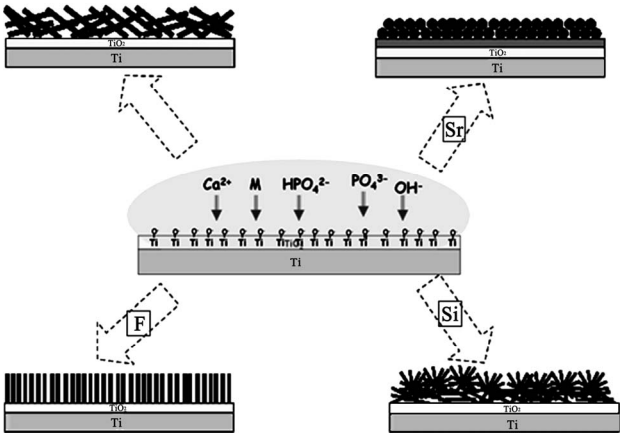

Figure 6. Schematic illustration of ion substituted hydroxyapatite coatings with different morphology on the TiO2/Ti substrates.

Table 2. Crystal size and crystallinity of HA, SrHA, SiHA and FHA reflected by XRD patterns.

Sample	Line width (002) FWHM (2θ)	Average crystal size d (nm)	Crystallinity (X_c)
HA-37-2W	25.9963	35.58	0.0185
SrHA-37-2W	25.3722	16.27	0.199
FHA-37-2W	25.9395	25.10	0.0186
SiHA-37-2W	26.0015	25.45	0.0185

5. Conclusions

A simple method for the preparation of ion substituted hydroxyapatite coatings with controlled topography and composition was explored in this study. The results showed that the surface structure could be modified by substituting different ions into the apatite structure. The strontium, fluoride and silicon substituted hydroxyapatite coatings gave spherical, needle-like, and nano-flake-like morphologies which were very different to pure hydroxyapatite. The concentration of strontium ions was also found to affect the morphology of the coatings. The lower Sr concentration resulted in irregular and porous spherical particles and the higher one resulted in regular spherical particles. For the fluoride and silicon substituted coatings, there was no obvious difference between a high ion concentration and a low one. After ion substitution, the biomimetic hydroxyapatite coatings showed a poor crystallinity, and the crystal size decreased. XPS analysis showed that the atomic concentration of ions in the final coating was affected by the ion concentration in the PBS solution. A high ion concentration could result in higher amounts of substitutions. The surface composition analysis also showed that the highest amount of substitutions was achieved using strontium ions, followed by the fluoride ions and finally the silicon ions. In summary, the surface composition and morphology of hydroxyapatite produced via a biomineralization method can be controlled using ion substitutions.

6. Acknowledgements

This work was supported by BIOMATCELL, VINN Excellence Center of Biomaterials and Cell Therapy.

REFERENCES

[1] L. L. Hench, "Bioceramics: From Concept to Clinic," *Journal of the American Ceramic Society*, Vol. 74, No. 7,

July 1991, pp. 1487-1510.

[2] T. Kokubo, "Bioceramics and Their Clinical Applications," CRC Press, USA, 2008.

[3] J. E. Ellingsen and S. P. Lyngstadaas, "Bio-Implant Interface: Improving Biomaterials and Tissue Reactions," CRC Press, USA, 2003.

[4] R. Batzer, Y. Liu, D. L. Cochran, S. Szmuckler-Moncler, D. D. Dean, B. D. Boyan and Z. Schwartz, "Prostaglandins Mediate the Effects of Titanium Surface Roughness on MG63 Osteoblast-Like Cells and Alter Cell Responsiveness to 1 Alpha,25-$(OH)_2D_3$," *The Journal of Biomedical Materials Research*, Vol. 41, No. 3, September 1998, pp. 489-496.

[5] C. H. Lohmann, J. R. Sagun, V. L. Sylvia, D. L. Cochran, D. D. Dean, B. D. Boyan and Z. Schwartz, "Surface Roughness Modulates the Response of MG63 Osteoblast-Like Cells to 1,25-(OH)(2)D(3) Through Regulation of Phospholipase A(2) Activity and Activation of Protein Kinase A," *The Journal of Biomedical Materials Research*, Vol. 47, No. 2, November 1999, pp. 139-151.

[6] A. S. G. Curtis, "Small is Beautiful but Samller is the Aim: Review of a Life of Research," *Europe Cell & Mater*, Vol. 8, No. 22, October 2004, pp. 27-36.

[7] A. S. G. Curtis and P. Clark, "The Effect of Topographic and Mechanical Properties of Materials on Cell Behaviour," *Critical Reviews in Biocompatibility*, Vol. 5, 1990, pp. 343-362.

[8] L. Chou, J. D. Firth, V.-J. Uitto and D. M. Brunette, "Substratum Surface Topography Alters Cell Shape and Regulates Fibronectin mRNA level MRNA Stability Secretion and Assembly in Human Fibroblastes," *Journal of Cell Science*, Vol. 108, April 1995, pp. 1563-1573.

[9] M. Vallet-Regí, "Ceramics for Medical Applications," *Journal of Chemical Society, Dalton Transactions*, 2001, pp. 97-108.

[10] F. H. Lin, Y. S. Hsu, S. H. Lin and J. S. Sun, "The Effect of Ca/P Concentration and Temperature of Simulated Body Fluid on the Growth of Hydroxyapatite Coating on Alkali-Treated 316L Stainless Steel," *Biomaterials*, Vol. 23, No. 19, October 2002, pp. 4029-4038.

[11] X. Liu, P. Chu and C. X. Ding, "Surface Modification of Titanium, Titanium Alloys, and Related Materials for Biomedical Application," *Materials Sciences and Engineering Report*, Vol. 47, No. 3-4, December 2004, pp. 49-121.

[12] L. Sun, C. C. Berndt, K. A. Gross and A. Kucuk, "Material Fundamentals and Clinical Performance of Plasma-Sprayed Hydroxyapatite Coatings: A Review," *The Journal of Biomedical Materials Research*, Vol. 58, No. 5, 2001, pp. 570-592.

[13] H. Oonishi, L. Hench, J. Wilson, F. Sugihara, E. Tsuji, M. Matsuura, S. Kin, T. Yamamoto and S. Mizokawa, "Quantitative Comparison of Bone Growth Behavior in Granules of Bioglass, A-W Glass-Ceramic, and Hydroxyapatite," *The Journal of Biomedical Materials Research*, Vol. 51, No. 1, July 2000, pp. 37-46.

[14] D. Knaack, M. E. P. Goad, M. Aiolova, C. Rey, A. Tofighi, P. Chakravarthy and D. D. Lee, "Resorbable Calcium Phosphate Bone Substitute," *The Journal of Biomedical Materials Research*, Vol. 43, No. 4, 1998, pp. 399-409.

[15] C. P. A. T. Klein, A. A. Driessen, K. d. Groot and V. D. Hoof, "Biodegradation Behavior of Various Calcium Phosphate Materials in Bone Tissue," *The Journal of Biomedical Materials Research*, Vol. 17, No. 5, September 1983, pp. 769-784.

[16] C. Ergun, T. J. Webster, R. Bizios and R. H. Doremus, "Hydroxylapatite with Substituted Magnesium, Zinc, Cadmium, and Yttrium. I. Structure and Microstructure," *The Journal of Biomedical Materials Research Part A*, Vol. 59, No. 2, February 2002, pp. 305-311.

[17] R. A. Young and P. E. Mackie, "Crystallography of Human Tooth Enamel: Initial Structure Refinement," *Materials Research Bulletin*, Vol. 15, No. 1, January 1980, pp. 17-29.

[18] Z. Y. Li, W. M. Lam, C. Yang, B. Xu, G. X. Ni, S. A. Abbah, K. M. C. Cheung, K. D. K. Luk and W. W. Lu, Chemical Composition, Crystal Size and Lattice Structural Changes after Incorporation of Strontium into Biomimetic Apatite," *Biomaterials*, Vol. 28, No. 7, March 2007, pp. 1452- 1460.

[19] E. Canalis, M. Hott, P. Deloffre, Y. Tsouderos and P. J. Marie, "The divalent Strontium Salt S12911 Enhances Bone Cell Replication and Bone Formation *in vitro*," *Bone*, Vol. 18, No. 6, June 1996, pp. 517-523.

[20] J. Christoffersen, M. R. Christoffersen, N. Kolthoff and O. Barenholdt, "Effects of Strontium Ions on Growth and Dissolution of Hydroxyapatite and on Bone Mineral Detection," *Bone*, Vol. 20, No. 1, January 1997, pp. 47-54.

[21] A. M. Pietak, J. W. Reid, M. J. Stott and M. Sayer, "Silicon Substitution in the Calcium Phosphate Bioceramics," *Biomaterials*, Vol. 28, No. 28, October 2007, pp. 4023-4032.

[22] C. Robinson, R. C. Shore, S. J. Brookes, S. Strafford, S. R. Wood and J. Kirkham, "The Chemistry of Enamel Caries," *Critical Reviews in Oral Biology and Medicine*, Vol. 11, No. 4, 2000, pp. 481-495.

[23] Y. Wang, S. Zhang, X. Zeng, L. L. Ma, W. Weng, W. Yan and M. Qian, "Osteoblastic Cell Response on Fluoridated Hydroxyapatite Coatings," *Acta Biomater*, Vol. 3, No. 2, March 2007, pp. 191-197.

[24] E. Zhang and C. Zou, "Porous Titanium and Silicon-Substituted Hydroxyapatite Biomodification Prepared by a Biomimetic Process: Characterization and *In vivo* Evaluation," *Acta Biomater*, Vol. 5, No. 5, June 2009, pp. 1732-1741.

[25] W. Xue, H. L. Hosick, A. Bandyopadhyay, S. Bose, C. Ding, K. D. K. Luk, K. M. C. Cheung and W. W. Lue, "Preparation and Cell–Materials Interactions of Plasma Sprayed Strontium-Containing Hydroxyapatite Coating," *Surface & Coatings Technology*, Vol. 201, No. 8, January 2007, pp. 4685-4693.

[26] G. Qi, S. Zhang, K. A. Khora, W. Weng, X. Zeng and C. Liu, "An Interfacial Study of Sol–Gel-Derived Magne-

sium Apatite Coatings on Ti6Al4V Substrates," *Thin Solid Films*, Vol. 516, No. 16, June 2008, pp. 5172-5175.

[27] E. S. Thian, J. Huang, S. M. Best, Z. H. Barber and W. Bonfield, "Novel Silicon-Doped Hydroxyapatite (Si-HA) for Biomedical Coatings: An *In vitro* Study Using Acellular Simulated Body Fluid," *The Journal of Biomedical Materials Research Part B*: *Appl Biomater*, Vol. 76, No. 2, February 2006, pp. 326-333.

[28] E. L. Solla, P. Gonzalez, J. Serra, S. Chiussi, B. Leon and J. G. Lopez, "Pulsed Laser Deposition of Silicon Substituted Hydroxyapatite Coatings from Synthetical and Biological Sources," *Applied Surface Science*, Vol. 254, No. 4, December 2007, pp. 1189-1193.

[29] Y. Han, D. H. Chen and L. Zhang, "Nanocrystallized SrHA/SrHA–$SrTiO_3$/$SrTiO_3$–TiO_2 Multilayer Coatings Formed by Micro-Arc Oxidation for Photocatalytic Application," *Nanotechnology*, Vol. 19, No. 33, July 2008, pp. 335-705.

[30] H. B. Wen, J. R. D. Wijin, F. Z. Cui and K. D. Groot, "Preparation of Calcium Phosphate Caotings on Titanium Implant Materials by Simple Chemistry," *The Journal of Biomedical Materials Research*, Vol. 41, No. 2, Auguest 1998, pp. 227-236.

[31] J. Forsgren, F. Svahn, T. Jarmar and H. Engqvist, "Formation and Adhesion of Biomimetic Hydroxyapatite Deposited on Titanium Substrates," *Acta Biomaterialia*, Vol. 3, No. 6, November 2007, pp. 980-984.

[32] W. Xia, C. Lindahl, J. Lausmaa, P. Borchardt, A. Ballo, P. Thomsen and H. Engqvist, "Biomineralized Strontium Substituted Apatite/Titanium Dioxide Coating on Titanium Surfaces," *Acta Biomaterialia*, Vol. 6, No. 4, April 2010, pp. 1591-1600.

[33] D. V. Vasudev, J. L. Ricci, C. Sabatino, P. J. Li and J. R. Parsons, "*In vivo* Evaluation of a Biomimetic Apatite Coating Grown on Titanium Surfaces," *The Journal of Biomedical Materials Research Part A*, Vol. 69, No. 4, June 2004, pp. 629-636.

[34] F. He, G. Yang, X. Wang and S. Zhao, "Bone Responses to Rough Titanium Implants Coated with Bjiomimetic Ca-P in Rabbit Tibia," *The Journal of Biomedical Materials Research Part B*, Vol. 90, No. 2, August 2009, pp. 857-863.

[35] R. Hazan, R. Brener and U. Orun, "Bone-Growth to Metal Implants is Regulated by Their Surface Chemical Properties," *Biomaterials*, Vol. 14, No. 8, July 1993, pp. 570-574.

[36] A. Boyde, "Microstructure of Enamel," *Ciba doundation symposium* 205- *dental enamel*, John Wiley & Sons, New York, 1997.

[37] A. L. Oliveira, R. L. Reis and P. Li, "Strontium-Substituted Apatite Coating Grown on Ti6Al4V Substrate through Biomimetic Synthesis," *The Journal of Biomedical Materials Research Part B*, Vol. 83, No. 1, October 2007, pp. 258-265.

[38] J. Wang, Y. Chao, Q. Wan, Z. Zhu and H. Yu, "Fluoridated Hydroxyapatite Coatings on Titanium Obtained by Electrochemical Deposition," *Acta Biomaterialia*, Vol. 5, No. 5, June 2009, pp. 1798-1807.

[39] B. Bracci, P. Torricelli, S. Panzavolta, E. Boanini, R. Giardino and A. Bigi, "Effect of Mg^{2+}, Sr^{2+}, and Mn^{2+} on the Chemico-Physical and *in vitro* Biological Properties of Calcium Phosphate Biomimetic Coatings," *Journal of Inorganic Biochemistry*, Vol. 103, No. 12, December 2009, pp. 1666-1674.

